JOURNAL OF Materials Feature Article CHEMISTRY

Fast oxygen ion conductors—from doped to ordered systems†

Truls Norby*

Department of Chemistry, University of Oslo, Centre for Materials Science, Gaustadalleen 21, Oslo, Norway N-0349. E-mail: trulsn@kjemi.uio.no; Fax: +47-22958749

Received 2nd May 2000, Accepted 13th July 2000
First published as an Advance Article on the web 10th October 2000

This contribution briefly introduces the traditional acceptor doping of oxides, charge compensated by oxygen vacancies to bring about the oxygen ion conduction utilised in solid oxide electrolytes. It is next shown how a simple defect–chemical approach to defect–defect interactions is a useful first-approximation tool in the interpretation of data and design of improved materials, *e.g.* by optimising dopants. Moreover, it is shown how the trapping of vacancies at acceptor defects can be avoided altogether if the cation sublattice can be made to order completely. This is realised in a few known systems and we illustrate the principle using the oxygen deficient complex perovskite $Sr_4(Sr_2Nb_2)O_{11}$ as an example, in which the Sr and Nb on the B-site sublattice can be perfectly ordered into a NaCl-structure-type arrangement, leaving all oxygen ion sites equivalent, without trapping sites. The design of new materials should thus aim at cation order, and the possibility of achieving this is discussed also for pyrochlore type oxides. A Kröger–Vink type notation for an inherently deficient sublattice without defects in the other sublattices is proposed.

Introduction

Since the discoveries of solid state oxygen ion conductors, *e.g.*, in the form of Y-substituted ZrO_2, the principle of substituting in a lower valent cation to form charge compensating oxygen vacancies has become the standard route to oxygen ion conducting electrolytes. Many systems have since been investigated, and several oxides with superior oxygen ion conduction have been and are being identified, both electrolytes (*e.g.* Gd-doped CeO_2 and Sr+Mg-doped $LaGaO_3$) and mixed conductors (*e.g.* Sr-doped $LaCoO_3$ and Fe-doped $SrTiO_3$). We will look at the principles behind this doping strategy in very simple ways and see how oxygen vacancy conductivity normally is suppressed at large defect concentrations, caused by defect interactions and ordering. However, by following the behaviour of an untypical example, we will show that order can be turned to our advantage if we are able to order the charge deficient cation sublattice without ordering the accompanying anion defects.

The ideal, acceptor substituted oxide

In an acceptor substituted oxide, where the acceptors are compensated by oxygen vacancies, $V_O^{\cdot\cdot}$, the electroneutrality requires that the effective charges of the vacancies correspond to those of the acceptors, and in terms of concentration it reads:

$$2c_{V_O^{\cdot\cdot}} = c_{Ml_M'} = \text{constant} \quad (1)$$

where Ml_M' is a lower valent acceptor substituent at the site of a host metal M. The concentration of oxygen vacancies is the product of the site density of oxygen ions and the fraction of vacancies: $c_{V_O^{\cdot\cdot}} = c_O[V_O^{\cdot\cdot}]$. The oxygen vacancy conductivity is the product of the vacancies charge, concentration, and charge mobility u, and the vacancy conductivity is thus in principle proportional to the dopant concentration; as has been confirmed in many systems at moderate dopant levels and high temperatures.

$$\sigma_{V_O^{\cdot\cdot}} = 2ec_{V_O^{\cdot\cdot}}u_{V_O^{\cdot\cdot}} = 2ec_O[V_O^{\cdot\cdot}]u_{O^{\cdot\cdot}} = ec_{Ml_M'}u_{V_O^{\cdot\cdot}} \quad (2)$$

The mobility of vacancies is in principle proportional to the probability that a neighbouring site is occupied, and thus the mobility contains the factor $1-[V_O^{\cdot\cdot}]$.[1] This will in itself give a maximum in the conductivity *vs.* acceptor doping content at a level corresponding to $[V_O^{\cdot\cdot}]=1/2$, although this is not reached in practice in oxygen ion conducting oxides. For small dopant and defect levels, this term can be neglected, and the mobility considered independent of vacancy concentration.

In the case we have described, the temperature dependence of the conductivity only reflects that of the mobility of vacancies:

$$\sigma_{V_O^{\cdot\cdot}} = 2ec_O[V_O^{\cdot\cdot}](1-[V_O^{\cdot\cdot}])u^0_{V_O^{\cdot\cdot}}\frac{1}{T}\exp\left(\frac{-\Delta H_m}{kT}\right) \quad (3)$$

where ΔH_m is the activation energy of the mobility (and self diffusion) of vacancies, $u^0_{V_O^{\cdot\cdot}}$ is the pre-exponential of the mobility (at $[V_O^{\cdot\cdot}]=0$) and the $1/T$ term arises through the Nernst–Einstein relation between mobility and random diffusion. Thus, for an acceptor-dominated, pure oxygen vacancy conductor, ΔH_m is typically reported from the slope of the (ideally) straight line of a plot of $\ln(\sigma T)$ *vs.* $1/T$. It can also be obtained from an Arrhenius plot of the oxygen diffusivity ($\ln D_O$ *vs.* $1/T$). It can *not* be obtained from a plot of $\ln\sigma$ (or $\log\sigma$) *vs.* $1/T$, which should *not* be a fully straight line and *typically* would give a value of ΔH_m which is around 10 kJ mol^{-1} (0.1 eV) too small. Nevertheless, the *presentation* of the conductivity can be done well in a $\log\sigma$ *vs.* $1/T$ plot, as this is more intelligible than $\ln(\sigma T)$ or $\log(\sigma T)$ plots in terms of the actual value of the conductivity.

Defect interactions

At increasing levels of dopants and charge compensating point defects, one may expect non-idealities, and it was soon found for most systems that the conductivity goes through a maximum as a function of dopant content (at levels far below that predicted from the $1-[V_O^{\cdot\cdot}]$ term). Furthermore, the conductivity usually deviates from the Arrhenius-like behaviour of eqn. (3) and exhibits an increasing activation enthalpy with decreasing temperature. This behaviour has been given various physical interpretations including changes in the lattice

†Basis of a presentation given at Materials Discussion No. 3, 26–29 September, 2000, University of Cambridge, UK.

DOI: 10.1039/b003463k

parameter and other variations in the structure, defect structure changes, trapping and other defect–defect interactions, and defect ordering. These are, in turn, described mathematically with various degrees of sophistication, ultimately only approachable by computer simulation techniques.

In a simple approach, each vacancy can be considered to be attracted by and trapped at a site neighbouring or at least close to an acceptor. This is often conceived as due to coulomb attraction, but it is probably more correct to view it simply as an overall decrease in the lattice energy (as this will not preclude the possibility of, *e.g.*, vacancy–vacancy association which is the basis for many types of ordering).

The diffusion of the vacancy trapped to an immobile acceptor dopant will now have to include an extra activation enthalpy each time the vacancy is to get freed from its captor. One can approach this by analysing the diffusion in terms of normal jumps and de-trapping jumps, with different activation energies.

An alternative approach, probably to be considered as even simpler, is based on defect chemistry. In this we consider all trapped (associated) vacancies as immobile, all un-associated vacancies as mobile, and the concentration of the two types a matter of a simple defect–chemical reaction:

$$V_O^{\cdot\cdot} + Ml_M^{\prime} = (V_O Ml_M)^{\cdot} \tag{4}$$

At equilibrium, and assuming ideality, we have:

$$K_a = \exp\left(\frac{\Delta S_a}{R}\right)\ \exp\left(\frac{-\Delta H_a}{RT}\right) = \frac{[(V_O Ml_M)^{\cdot}]}{[Ml_M^{\prime}][V_O^{\cdot\cdot}]} \tag{5}$$

where the concentrations are in site fractions. The very simplest solution to the situation is to consider that the electroneutrality is:

$$2[V_O^{\cdot\cdot}]c_O + [(V_O Ml_M)^{\cdot}]c_M = [Ml_M^{\prime}]c_M \tag{6}$$

where we have chosen to let the concentration of the associate $(Ml_M V_O)^{\cdot}$ be represented by the site fraction with respect to the cation M sublattice. (The choice of reference lattice may change the pre-exponential of the mass action constant and the apparent entropy, but otherwise does not affect our treatment.) Furthermore, mass balance with respect to the acceptors is then given by:

$$[Ml_M^{\prime}] + [(V_O Ml_M)^{\cdot}] = [Ml_M]_0 = \text{constant} \tag{7}$$

and in an otherwise dilute solution model, we then obtain for the site fraction of free vacancies:

$$[V_O^{\cdot\cdot}] = \frac{-(A+2) + \sqrt{\{A^2 + 12A + 4\}}}{4K_a} \tag{8}$$

where $A = K_a[Ml_M]_0 c_M/c_0$. This derivation neglects the possibility of the double associates $(V_O Ml_M V_O)^{\cdots}$ and $(Ml_M V_O Ml_M)^{x}$ and of more advanced site exclusion principles. It thus represents a first approximation to the problem.

Eqn. (8) has two limiting cases: at relatively high temperatures and low dopant concentrations, practically all vacancies are free; their concentration is almost independent of temperature, given only by the dopant level. At relatively low temperatures and high dopant levels, on the other hand, practically all vacancies are trapped. The concentration of free vacancies then decreases with decreasing temperature and becomes independent of dopant level.

Fig. 1 shows $[V_O^{\cdot\cdot}]$ from eqn. (8) plotted *vs.* $1/T$ in an arbitrary case, with three different negative values of ΔH_a. Fig. 2 shows the same for three different values of ΔS_a. While ΔH_a is often considered the parameter of prime importance, it is noteworthy that a modest value of ΔS_a also makes a difference. If positive it may cause substantial association even at very high temperatures or small ΔH_a values. Conversely, a negative ΔS_a may shift

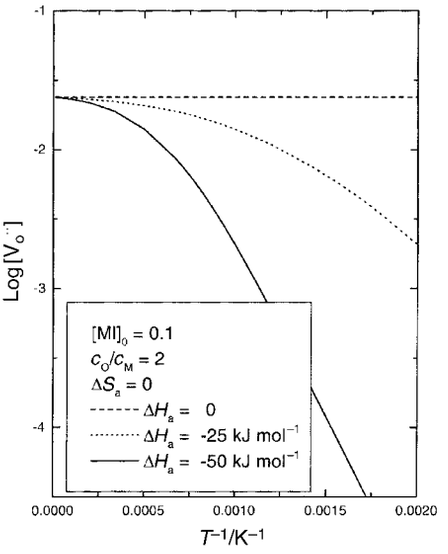

Fig. 1 Fraction of free oxygen vacancies (over all oxygen sites) *vs.* inverse temperature (500–∞ K) for an oxide MO_2 doped with 10% Ml^{3+} for $\Delta S_a = 0$and at three different values of ΔH_a.

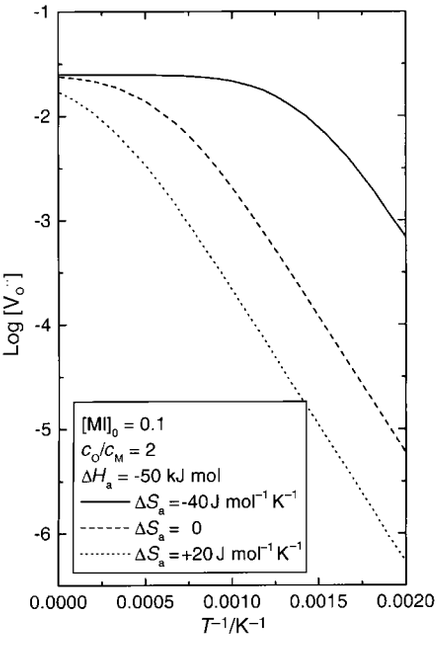

Fig. 2 Fraction of free oxygen vacancies (over all oxygen sites) *vs.* inverse temperature (500–∞ K) for an oxide MO_2 doped with 10% Ml^{3+} for $\Delta H_a = -50$ kJ mol^{-1} and at three different values of ΔS_a.

association to lower temperatures and help maintain a high vacancy mobility.

Fig. 3 shows a plot of $[V_O^{\cdot\cdot}]$ *vs.* the dopant concentration (from 1 to 100%) according to eqn. (8). It shows that the association causes the concentration of free vacancies to level out at a plateau given by temperature, ΔH_a, and ΔS_a.

The fraction of unassociated, mobile vacancies from eqn. (8) can be inserted into the factor $[V_O^{\cdot\cdot}]$ in eqn. (3) above for the conductivity, whereas the factor $1-[V_O^{\cdot\cdot}]$ (if not neglected) should contain not only the free, but all vacancies, and can thus be conveniently replaced by a term $1-[V_O^{\cdot\cdot}]_0 = 1-[Ml_M]_0 c_M/c_O$:

$$\sigma_{V_O^{\cdot\cdot}} = 2ec_O[V_O^{\cdot\cdot}](1-[Ml_M]_0 c_M/c_O)u^0_{V_O^{\cdot\cdot}}\ \frac{1}{T}\ \exp\left(\frac{-\Delta H_m}{kT}\right) \tag{9}$$

Fig. 4 shows an example of the temperature dependence of

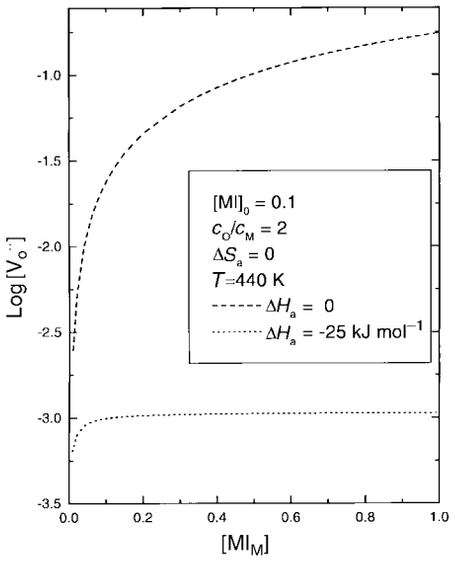

Fig. 3 Fraction of free oxygen vacancies (over all oxygen sites) for an oxide MO_2 *vs.* content of MI^{3+} acceptor for $\Delta S_a=0$ and at three different values of ΔH_a. $T=440$ K.

the conductivity (as $\log(\sigma T)$ *vs.* $1/T$) according to eqns. (8) and (9), obviously showing a bend as association effectively sets in, so that the activation enthalpy at low temperatures is the sum of ΔH_m and ΔH_a. (Note that it is necessary to plot $\log(\sigma T)$ rather than $\log \sigma$ in order to obtain anything near linear parts of the curves above and below the association changeovers.)

Fig. 5 shows the conductivity isotherm *vs.* dopant concentration. Now, the $1-[MI_M]_0 c_M/c_O$ term causes the case with heavy association to go through a maximum.

The fitting of experimental data to this simple kind of model works reasonably well in many cases, especially when the defect concentrations are not too large and the temperatures not too low. Fig. 6 shows results from our own laboratory[2] of the ac conductivity of three compositions of Sr + Mg-doped $LaGaO_3$ fitted to a model like the one we have described here. The results are in perfect agreement with SIMS ^{18}O diffusivity measurements on one of the compositions and do not differ much from the results of others on similar compositions. The fit results for the three compositions fell within $\Delta H_m=50\pm5$kJ mol^{-1}, $\Delta H_a=-65\pm5$ kJ mol^{-1}, and

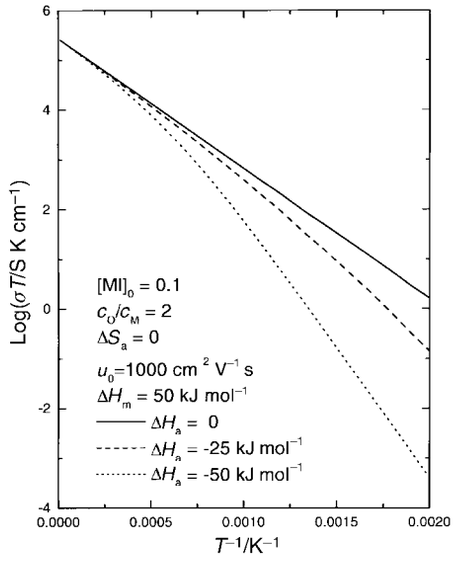

Fig. 4 $\text{Log}(\sigma T)$ *vs.* $1/T$ (500–∞ K) for an oxide MO_2 doped with 10% MI^{3+} for $\Delta H_m=50$kJ mol^{-1}, $\Delta S_a=0$, and at three different values of ΔH_a.

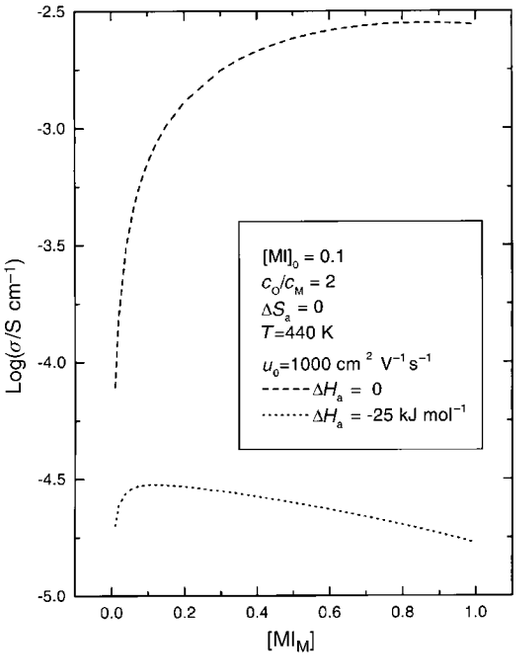

Fig. 5 Log σ *vs.* content of MI^{3+} acceptor for $\Delta S_a=0$ and at three different values of ΔH_a. $T=440$ K, $\Delta H_m=50$ kJ mol^{-1}, $\Delta S_a=0$.

$\Delta S_a=-40\pm10$ J mol K^{-1} for the simple model used. It is important to emphasise that this is but one, and the simplest, of several possible models. (Alternative models comprise structural changes and vacancy clustering.)[3] Thus, the fit parameters obtained should not be given too much weight at this stage. Nevertheless, with the fairly large association enthalpy it is tempting to consider the possibility that it is actually the considerable negative entropy obtained here that may be responsible for the high conductivity of this material, *cf.* Fig. 2.

Fig. 7 shows conductivities of rare-earth doped CeO_2 *vs.* dopant contents. (The measured data are taken at low temperatures where the effect of dopants is pronounced, and where bulk resistance is easily delineated from grain boundary resistance by impedance spectroscopy). The characteristic maxima and curve shapes in Fig. 7 resemble the curves predicted from our model (Fig. 5). However, the real dependencies are typically stronger upon dopant content at both sides of the maxima. On the low-content side, this may be attributed to activation energies decreasing with doping. This is common and may reflect lattice parameter and other structural changes and also a changeover from intrinsic to extrinsic defect dominance. On the high-content side of the maximum, the large dependency may reflect more severe defect–defect interactions and ordering phenomena than accounted for in

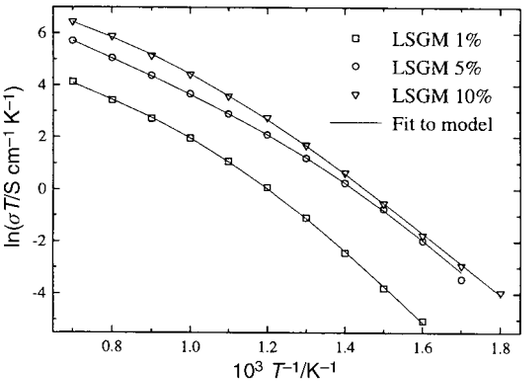

Fig. 6 $\text{Log}(\sigma T)$ *vs.* $1/T$ for $La_{1-x}Sr_xGa_{1-x}Mg_xO_{3-x/2}$ for $x=0.01$, 0.05 and 0.1. Lines are fits to a model for association as described in the text. Reprinted with permission from ref. 2.

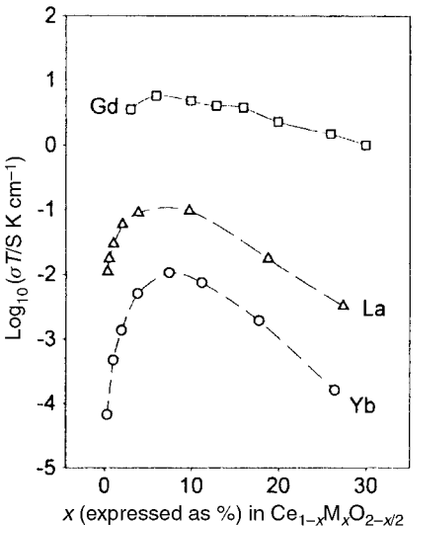

Fig. 7 Log(σT) *vs.* dopant content in rare-earth-doped CeO_2. Gd-doped sample data taken at 500 K, La- and Yb-doped samples data taken at 440 K. Reprinted with permission from ref. 1.

our simple model. It appears that the simple model we have excercised thus works best at intermediate dopant contents (and high temperatures), *i.e.*, where the conductivities and research efforts are highest.

In order to take into account larger defect clusters and defect interactions on longer length-scales one will generally need to use computer simulation techniques. These show that in ZrO_2 (see Fig. 8)[4] and CeO_2[5] the binding energies between acceptor and vacancy are highest for nearest-neighbour positions for small rare earth dopants and next-nearest neighbour positions for the largest rare earths. The smallest activation energy and highest value for the oxygen vacancy mobility appears at the crossover. These and other investigators' calculations[6] also show a higher binding energy for double associates $(\mathrm{Ml_M V_O Ml_M})^x$ which helps explain how the conductivity and phase stability is reduced beyond that predicted by the simple model at high dopant contents. For recent reviews with various focii on these and related aspects of oxygen ion conduction in oxides in general and ceria in particular, see, for instance, refs. 1,7,8,9.

In order to successfully delineate the diffusivity into terms of

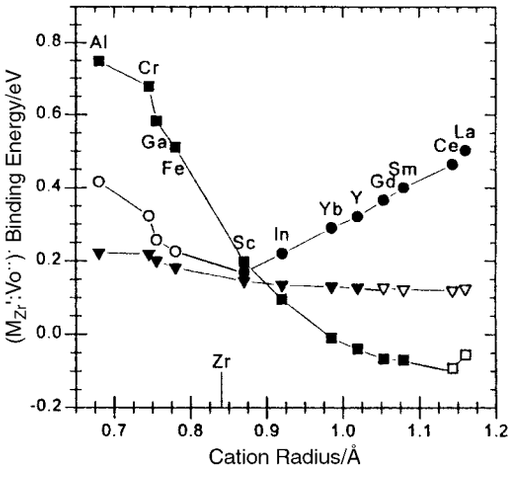

Fig. 8 Atomistic simulation of binding (association) energy between vacancy and acceptor in ZrO_2 as a function of acceptor radius. Nearest-neighbour binding (■) largest for small acceptors, next-nearest neighbour (●) largest for big acceptors. Optimum dopant is expected to be at the minimum. Next-next-neighbour positions are also included (▽). Open symbols represent artificially stabilised configurations. Reprinted with permission from ref. 4.

trapping and free defect migration (at the least) one has to be able to monitor the bulk ionic transport process over a fairly large span of temperature and/or doping. If this is not possible, it is still useful to realise that association effects may be in operation, in order to ensure constructive interpretation of transport data. The author would like to encourage the use of a simple model such as the one above rather than to neglect association altogether in fear of the full complexity involved.

As we gain better control of the concentration of mobile vacancies it is getting clear that the mobility (or diffusivity) and its activation energy for these vacancies vary little between different compounds within the same structural group. For instance, a number of $LaMO_3$ perovskites with different dopings all have vacancy diffusivities less than an order of magnitude apart, and with comparable activation energies.[10] Similar behaviour, but with other values, is found within fluorite-related structures. One route to higher ionic conductivity thus clearly lies in the concentration of mobile vacancies through acceptor doping and the optimisation of dopants in order to minimize association. Examples are found in the optimisation of rare earth dopants in fluorite oxides (Sc^{3+} in ZrO_2[4] and Gd^{3+} in CeO_2[5,7,8]) and the development of $Sr^{2+}+Mg^{2+}$-doping for $LaGaO_3$ and later on the replacement of Mg^{2+} by Co^{2+}.[11]

Inherently defective, disordered systems

Some compounds without dopants at all, and with inherently defective disordered structures, are found to have considerably lower activation energies of diffusion and conduction than doped systems. For example, the classical material δ-Bi_2O_3, with a fluorite-type structure, has only around 0.3 eV of activation energy for vacancy transport, the same, by the way, as the disordered proton conductor $CsHSO_4$, and mainly the same as activation energies in liquid electrolytes.

Similarly, disordered oxygen vacancies with high diffusivities and correspondingly low activation energies of around 0.5 eV are found in the high-temperature perovskite phases of $Sr_2Fe_2O_5$[12] and $Ba_2In_2O_5$.[13]

If we wish, the disordered and highly oxygen ion conducting phases of Bi_2O_3, $Sr_2Fe_2O_5$, and $Ba_2In_2O_5$ mentioned above may be seen as, for instance, ZrO_2, $SrZrO_3$, and $BaZrO_3$ in which Zr is substituted 100% with, respectively, Bi, Fe, and In, and compensated by oxygen vacancies. From this we get a hint that while acceptors in large concentrations trap vacancies, the trapping may disappear if we are able to reach a compound where the acceptors are no longer foreign to their sublattice. Nevertheless, all the mentioned compounds still undergo disorder–order phase transitions upon cooling from high temperatures, whereby they lose their high ionic conductivities.

Order and disorder

In both classes of oxide ion conductors described above (doped and inherently defective systems) we associate high vacancy mobility with disorder: A disordered, random solution of acceptor substituents to be compensated by unassociated oxygen vacancies, or, a disordered amount of originally ordered inherent oxygen vacancies.

No doubt, in our quest for high oxygen transport, the desire for a disordered oxygen sublattice remains. But this is often taken to carry over to the cation sublattice(s). We shall see that this needs not be the case, that order and disorder in the cation and anion sublattices can be independent of each other, and that cation disorder is mainly a disadvantage if we can have oxygen disorder without it. We shall use perovskite-related and pyrochlore systems in our examples in the following.

Order/disorder in the perovskite-related system $Sr_3(Sr_{1+x}Nb_{2-x})O_{9-3x/2}$ $(0 \leqslant x \leqslant 0.5)$

The compound $Sr_3(SrNb_2)O_9$ is related to many similarly composed complex perovskite-related electroceramics, but is remarkable in that the large Sr^{2+} ion here occupies part of the small, octahedrally coordinated B-sites in the perovskite structure. In the stoichiometric composition, all oxygen sites are occupied, and the B-site cations are ordered into the so-called 2 : 1 structure which may be seen as two Sr + Nb layers alternating with one Nb-only layer. As we increase the Sr content, the Sr : Nb ratio on the B-site increases. Thus, the average charge on the B-site decreases, and oxygen vacancies are introduced for charge compensation. The electroneutrality condition can be approximated as $2[V_O^{\cdot\cdot}] = 3[Sr'_{Nb}] = 2[Sr''_B]$, where the two acceptor defect representations arise from different choices of host site (Nb^{5+} sites or average B^{4+} sites).

The material becomes an oxygen vacancy conductor, and the ionic conductivity increases with Sr excess. At moderate temperatures, the material picks up water and becomes a protonic conductor,[14] but that will not be our concern here. During our studies mainly of protonic conduction in the system, however, it was established that the oxygen ion conduction not only increased with Sr excess, it increased much more than expected. At low Sr excesses it was approximately proportional to the Sr content, but then increased exponentially towards the end-member $Sr_3(Sr_{1.5}Nb_{1.5})O_{8.25}$, as evident from the plot in Fig. 9. There was thus in this sense little resemblance to the acceptor–vacancy associations or vacancy–vacancy ordering commonly seen in most other doped systems. The end-member has 1 out of 12 oxygen ions missing and is more conveniently written $Sr_4(Sr_2Nb_2)O_{11}$; after proper high temperature annealing it exhibits a very high ionic conduction with a small activation energy of around 0.4 eV down as low as 400 °C and thus no sign of association, see Fig. 10. (By annealing at intermediate temperatures the conductivity nevertheless slowly degrades as the situation that sustains the high conductivity breaks down in some way.)

What goes on in this system to give such a high mobility of the vacancies as the acceptor concentration increases? The pseudo-cubic lattice constant increases linearly, from around

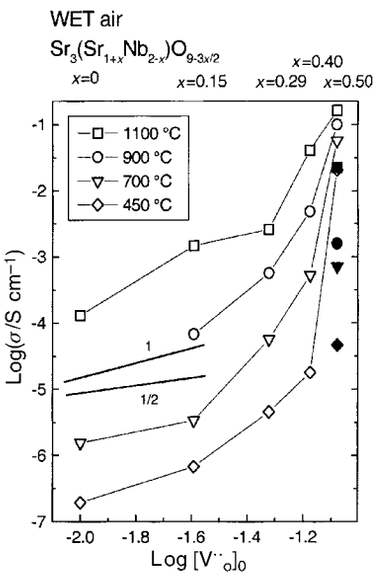

Fig. 9 Total conductivity of $Sr_3(Sr_{1+x}Nb_{2-x})O_{9-3x/2}$ *vs.* vacancy fraction at different temperatures in wet air. Filled symbols represent conductivity of end composition ($=Sr_4(Sr_2Nb_2)O_{11}$) without proper annealing (and include a high proportion of proton conduction at the lowest temperatures). Slopes indicated for comparison. Reprinted with permission from ref. 14.

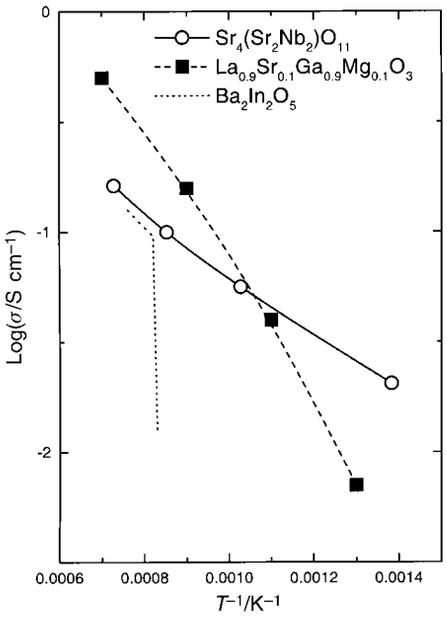

Fig. 10 Total (mainly ionic) conductivity of $Sr_4(Sr_2Nb_2)O_{11}$ (extracted from the previous figure) in comparison with 10% Sr,Mg-doped $LaGaO_3$[2] and $Ba_2In_2O_5$.[13] Values for $Sr_4(Sr_2Nb_2)O_{11}$ and $Ba_2In_2O_5$ may be on the low side due to use of the two-point technique as compared to the four-point technique used for $LaGaO_3$.

8.265 Å to around 8.31 Å, not a sufficiently large effect to rationalise the dramatic increase in conductivity. In their study of proton conduction in $Ba_3(Ca_{1+x}Nb_{2-x})O_{9-3x/2}$ ("BCN") and related materials, Du and Nowick[15] found that BCN materials had undergone a change from the 2 : 1 to the 1 : 1 type of ordering in the B-site cations when the Ca excess had reached 18%, and the samples with this and higher Ca contents exhibited a higher proton mobility than those with lower Ca contents. We assume that the same goes on in our system; neutron diffraction, X-ray diffraction, and electron diffraction on the $Sr_4(Sr_2Nb_2)O_{11}$ end member are all in agreement with this (although neither method can unambiguously position all cations in the structure).

Irrespective of details, the system starts out at $x = 0$ with some Sr–O–Nb and some Nb–O–Nb configurations. As the Sr excess, x, increases, there are more Sr–O–Nb configurations, but also Sr–O–Sr in the disordered B-site cation planes. As we approach $x = 0.5$ the structure takes on the 1 : 1 ordering in which Sr and Nb occur in such a way that the B-site lattice can be seen as a NaCl structure-type arrangement. Now, we only have Sr–O–Nb arrangements.

We have thus a lattice of alternating SrO_6 and NbO_6

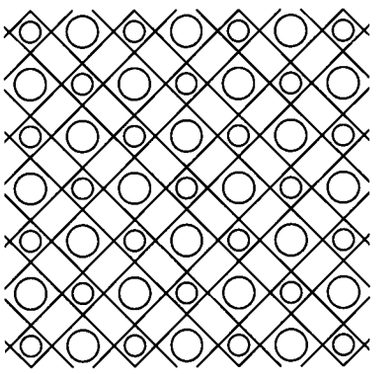

Fig. 11 Schematic illustration of the 1 : 1 ordering in $Sr_4(Sr_2Nb_2)O_{11}$, with alternating small Nb and large Sr octahedra (exaggerated size difference). Oxygen ions (and vacancies) are not shown, but occupy all line crosspoints (which are all equivalent).

octahedra; very different in bond-lengths and size, but this can otherwise be well accommodated in the 1 : 1 ordering, as depicted two-dimensionally in Fig. 11.

However, the oxygen vacancies, by all landmarks, remain disordered. As all positions are now equivalent, there are no traps (as in normal acceptor doped cases) and the vacancy mobility and the conductivity become very high.

One can imagine that annealing at the right temperature is essential to obtain the high conductivity: Insufficient annealing or too high a temperature may render the cations disordered, thereby creating Sr–O–Sr vacancy traps and Nb–O–Nb vacancy migration obstacles. On the other hand, too low a temperature may order the oxygen vacancies (probably requiring a rearrangement of cations as well). It is thus, in retrospect, not surprising that the $x=0.5$ end member first turned out to have a disappointingly low conductivity (included in Fig. 9) until we learned to anneal it properly.

With x close to, but still below 0.5, there will be occasional Nb–O–Nb configurations; these will impose distortions to the lattice and traps and hinder oxygen vacancy migration, and the conductivity drops sharply as the Sr excess falls below 0.5.

We would like to add that much the same behaviour and dependency on the Sr content is found also for the $Sr_3(Sr_{1+x}Ta_{2-x})O_{9-3x/2}$ system.[16] These systems have limited practical interest due to their high basicity and poor thermochemical stability towards CO_2 and H_2O, but they are instructive and inspiring as they exemplify high oxygen ion conduction along new routes.

Are we able to devise new perovskite-related oxides with high oxygen vacancy concentration and possibly high mobility as a result of ordering of the charge deficient cation sublattice? The example above has shown the utilisation of pentavalent B-site cations. If we instead consider uses of a tetravalent cation, like Ti^{4+}, we may for instance try to formulate an $A_4(B_2Ti_2)O_{11}$ phase, where A is an alkaline earth cation and B is a trivalent cation, and where we would hope for B : Ti ordering in a NaCl manner like in the Sr–Nb-case above. In order to do this we would want a large B^{3+} cation. Candidates are the larger lanthanoids, *e.g.*, Gd or Nd. The compound would be similar to $Ba_2YSnO_{5.5}$ recently reported to be a proton conductor in wet atmospheres.[17] The use of Ti may allow us to use a smaller A-site cation; possibly Ca, which is beneficial for the CO_2 tolerance.

Order and disorder in fluorite and pyrochlore systems

Consider adding an increasing amount of a fairly large trivalent cation like Nd^{3+} or Gd^{3+} to the oxide of a somewhat smaller tetravalent cation like Zr^{4+} in ZrO_2. The structure attains the cubic, fluorite structure at high temperature, randomly distributing both the acceptor dopant and oxygen vacancies. Oxygen vacancy conductivity first increases with doping. However, the vacancies and the acceptors eventually associate, and conductivity decreases and phase separation occurs.

If the trivalent rare earth is added in as much as a 1 : 1 ratio a new phase is formed, with the pyrochlore structure, *e.g.*, $Gd_2Zr_2O_7$ in which the cations are ordered. Furthermore, the anion sites of the fluorite-related structure are ordered into three different sites; 6 equivalent oxygen sites, denoted O(1), one differing oxygen site, denoted O(2), and one structurally empty site, denoted O(3).

The stoichiometric pyrochlore is at best a mediocre ionic conductor, relying on thermal creation of anion Frenkel defects (vacancies mainly on the 6 equivalent sites and interstices in the structural vacancies). The pyrochlores may be acceptor- or donor-doped to give a rich variety of conductivity enhancements (n- or p-type electronic or ionic)[18] but that is not our prime concern here.

However, if we heat the ordered, stoichiometric pyrochlores to sufficiently high temperatures, they may disorder. The ease with which they disorder depends mainly on the size difference, *i.e.*, the bigger the A : B size ratio, the less easily they disorder. $La_2Zr_2O_7$ does not disorder at any temperature, $Nd_2Zr_2O_7$ disorders to a defective fluorite only at around 2300 °C while $Gd_2Zr_2O_7$, with A and B cations much more similar in size, disorders at around 1500 °C. Ordering is sluggish, so the disordered states can often be quenched and characterised at ambient temperatures.

Those which disorder may then be viewed as 50% acceptor-doped fluorites. They exhibit high oxygen ion conductivities, but generally not higher than those of the same system with smaller contents of the acceptor (dilute solution range). This is as expected as we now have a very large concentration of disordered acceptors and vacancies which may associate extensively.

The interesting question is whether we can have partial order/disorder, as recently discussed by Wuensch *et al.*.[19] Upon heating the ordered system it appears that the 6 equivalent oxygen ions at O(1) positions and the vacant site O(3) may disorder first (by formation of anion Frenkel pairs) while the 7th ion at O(2) takes part first at a somewhat higher temperature. A similar behaviour is shown in Fig. 12 which summarises results from neutron diffraction studies of Heremans *et al.*[20] of the system $Y_2(Zr_yTi_{1-y})_2O_7$. As one increases the Zr content y the structure disorders, and the occupancy of O(1) decreases and that of the formerly empty O(3) increases somewhat before O(2) begins to participate.

Now to the important question of whether the cations at this stage have disordered or not. If they have, we are back at the heavily doped fluorite. But if they have not, we may see a higher vacancy mobility due to the regularity of the lattice and the equivalency of all sites. Fig. 12 indicates that cation disordering (A and B mixing) is relatively closely connected with anion disorder in the $Y_2(Zr_yTi_{1-y})_2O_7$ system.

A pyrochlore with ordered cations and disordered anions has to the author's knowledge not been reported. However, various sublattices within one structure may disorder independently, possibly as we have seen also in the pyrochlores, and the matter deserves further investigation. Keeping the cations ordered will require a relatively large size difference, while we also want to use rather large cations for polarisability and anion mobility. It might thus be of interest to investigate further III–IV pyrochlores with La, Pr, and Nd as A-site cations with various tetravalent anions at high temperatures. And it is certainly of interest to investigate II–V pyrochlores with Ca or Sr as A-site cations.

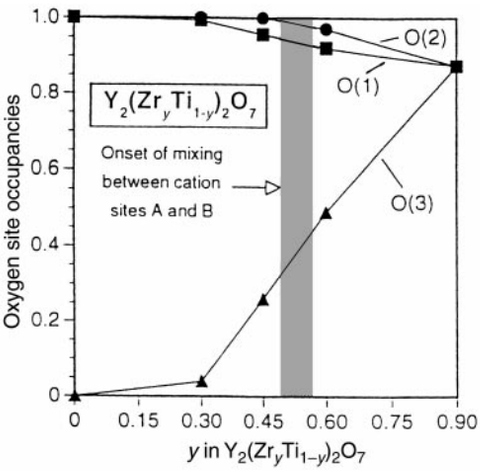

Fig. 12 Occupancies of different oxygen sites in the $Y_2(Zr_yTi_{1-y})_2O_7$ pyrochlore *vs.* Zr content y as determined by neutron diffraction. Reprinted with permission from ref. 20.

Defect notation in inherently deficient systems

We have described above the likely and possible settings where we have a deficiency in the oxygen sublattice but an ordered and therefore non-defective situation in the cation sublattice. Examples we have mentioned comprise the anion-disordered phases of $Sr_2Fe_2O_5$, $Ba_2In_2O_5$ (perovskites), $Sr_4(Sr_2Nb_2)O_{11}$ (complex perovskite) and δ-Bi_2O_3 (fluorite). If we were to describe the situation in these compounds in terms of defects, what would the formalism look like? There are basically three possibilities:

In the *anion-Frenkel approach*, we may see the disordered oxygen sublattice as a number of interstices on what used to be structurally empty sites and a corresponding number of vacancies on the structurally occupied sites. The electroneutrality would be $c_{V_O^{\cdot\cdot}} = c_{O_i''}$, and we would have such a large anion-Frenkel constant that the lattice would be saturated with defects and the defect concentrations would be fairly constant with temperature. However, one may not feel comfortable having to appoint interstitial and normal oxygen sites in a system now believed to contain equivalent sites.

In the *fully-acceptor-doped approach*, one considers that the compound is 100% substituted with an acceptor. Thus, $SrFeO_{2.5}$ might be seen as 100% Sr-substituted $LaFeO_3$ or 100% Fe-substituted $SrTiO_3$. Likewise, δ-Bi_2O_3 might be seen as 100% Bi-substituted ZrO_2. $Sr_3(Sr_{1.5}Nb_{1.5})O_{8.25}$ may be seen as Sr-substituted $Sr_3(SrNb_2)O_9$. and the electroneutrality then reads, for instance, $2c_{V_O^{\cdot\cdot}} = 3c_{Sr'_{Nb}} = \text{constant}$. Again, one may feel uncomfortable operating with an effectively charged acceptor defect in a perfect cation sublattice.

A third approach, applicable to *disordered inherently deficient sublattices*, has been forwarded lately by the author.[21,22,23] Here, one accepts the cation sublattice as perfect, and assigns a partially occupied oxygen site as a perfect one. For instance, the oxygen sites of the disordered δ-Bi_2O_3 and $Sr_2Fe_2O_5$ would be, respectively, 3/4 and 5/6 occupied. The oxygen sites in $Sr_4(Sr_2Nb_2)O_{11}$ would correspondingly be 11/12 occupied, with a real charge of −22/12 (= −11/6). In this framework, both the instantly empty and the instantly occupied sites are defects, and the electroneutrality reads:

$$11c_{V_{11/12O}^{11/6\cdot}} = c_{O_{11/12O}^{1/6'}} \tag{10}$$

which, naturally, expresses the ratio 1 : 11 of vacancies to oxygen ions. Redox equilibria may well be described in terms of these defects, *e.g.*:

$$V_{11/12O}^{11/6\cdot} + \frac{1}{2}O_2(g) = O_{11/12O}^{1/6'} + 2h^{\cdot} \tag{11}$$

and one may from this get the $[h^{\cdot}] = K_i/[e'] \propto p_{O_2}^{1/4}$ dependency, as usual.

The three approaches above all give basically the same physical result, and one may argue that the third "new" approach does not actually give anything that is new. However, it describes the situation without appointing defects in what really is a perfect cation lattice and without using an anion-Frenkel reaction to explain the anion disorder; the disorder did not arise from a defect reaction, but from a phase transformation.

Concluding remarks

We have pointed at the development of solid oxidic electrolytes by acceptor doping compensated by anion vacancies. In such solid solutions, association between the dopant and vacancy defects depresses the ionic conductivity at practical temperatures. The effect can be counteracted by optimising the acceptor dopant to fit the host lattice and/or be more polarisable, *e.g.* Gd^{3+} in CeO_2, Sc^{3+} in ZrO_2, and Co^{2+} in $LaGaO_3$. A simple theoretical treatment of association in terms of defect chemistry has been presented, and its application demonstrated in the analysis of oxygen ion conductivity variations.

Several examples are made of oxides which order their acceptors, normally to form new phases, and these are most often accompanied by ordering of the oxygen vacancies. Therefore, order as such is often seen as the thing to avoid in ionic conductors. However, we have also given examples of the occurence of systems with simultaneous cation order and a deficient, disordered anion sublattice, and in these one can avoid the trapping of oxygen vacancies, since there are in principle no cation defects. In binary oxides, this implies very high anion deficiencies, making their disorder highly unlikely, and δ-Bi_2O_3 with its small stability range is the only known example. Ternary oxides require less vacancies and more systems are known, *e.g.*, $BaInO_{2.5}$ and $SrFeO_{2.5}$. As the number of different cation sites increases, we actually get more possibilities of creating anion disorder without cation disorder, as the number of oxygen vacancies decreases to a more bearable level, examples being complex perovskites such as $Sr_4(Sr_2Nb_2)O_{11}$ and, as it seems, layered structures such as $Sr_4Fe_6O_{13}$.[22] The pyrochlore structure $A_2B_2O_7$ seems to offer similar possibilities to perovskites, and there are indications that the different occupied and vacant anion sites in some cases do disorder independently, but a clear cut example with an extraordinary oxygen vacancy conductivity has not been reported.

Anion deficiency and disorder, without cation defects, have been somewhat hard to describe in terms of typical Kröger–Vink defect notation, and an approach to facilitate this has been suggested.

We have suggested the search for new high ionic conductivity candidate systems among certain complex perovskites and among certain III–IV pyrochlores and in general among II–V pyrochlores. Both with respect to new and old systems our improved understanding will require a range of methods, preferably *in situ* (high temperature) for determination of structure, comprising the standard diffraction techniques (X-ray diffraction, neutron diffraction, and electron diffraction) for long range structure and order, but also *e.g.* EXAFS, Raman spectroscopy, and HRTEM for complementary information on short range order. Further, transport studies may comprise electrical conductivity measurements and tracer diffusion studies (notably ^{18}O diffusion by SIMS). ^{17}O-NMR can be a useful complementary technique.[9] Not least, however, we would like to stress the importance of checking the characteristics of the microstructure of any fast ionic conductor under test by analytical and high resolution electron microscopy and proper impedance spectroscopy. Good ionic conductors are easily missed if their conductance is masked by grain or domain boundary resistances, as has been the case *e.g.* with the protonic conduction of $BaZrO_3$.[24]

References

1 J. A. Kilner, *Solid State Ionics*, 2000, **129**, 13.
2 E. M. Ottesen, unpublished M.S. thesis, Department of Chemistry, University of Oslo, 1998 (in English).
3 P. R. Slater, J. T. S. Irvine, T. Ishihara and Y. Takita, *J. Solid State Chem.*, 1998, **139**, 135.
4 M. O. Zacate, L. Minervini, D. J. Bradfield, R. W. Grimes and K. Sickafus, *Solid State Ionics*, 2000, **128**, 243.
5 L. Minervini, M. O. Zacate and R. W. Grimes, *Solid State Ionics*, 1999, **116**, 339.
6 N. Sawaguchi and H. Ogawa, *Solid State Ionics*, 2000, **128**, 183.
7 M. Mogensen, N. M. Sammes and G. A. Tompsett, *Solid State Ionics*, 2000, **129**, 63.
8 B. C. H. Steele, *Solid State Ionics*, 2000, **129**, 95.
9 J. A. Reimer and S. B. Adler, in *Solid-state NMR spectroscopy of inorganic materials*, ed. J. J. Fitzgerald, American Chemical

Society, Washington DC, Symposium Series 717, 1999, p. 156.
10 J. Mizusaki, T. Kawada, Y. Nigara and K. Kawamura, *ISSI Lett. (ISSN0937-5961)*, 1999, **9**, 2.
11 T. Ishihara, H. Furutani, M. Honda, T. Yamada, T. Shibayama, T. Akbay, N. Sakai, H. Yokokawa and Y. Takita, *Chem. Mater.*, 1999, **11**, 2081.
12 A. Holt, T. Norby and R. Glenne, *Ionics*, 1999, **5**, 434.
13 J. B. Goodenough, J. E. Ruiz-Diaz and Y. S. Zhen, *Solid State Ionics*, 1990, **44**, 21.
14 R. Glöckner, A. Neiman, Y. Larring and T. Norby, *Solid State Ionics*, 1999, **125**, 369.
15 Y. Du and A. S. Nowick, *Mater. Res. Soc. Symp. Proc.*, 1995, **369**, 289.
16 I. Animitsa, A. Neiman, D. Dildin and S. Nohrin, *Solid State Ionics*, 2000, in print.
17 P. Murugaraj, K.-D. Kreuer, T. He, T. Schober and J. Maier, *Solid State Ionics*, 1997, **98**, 1.
18 H. Tuller, *Solid State Ionics*, 1992, **52**, 135.
19 B. J. Wuensch, K. W. Eberman, C. Heremans, E. M. Ku, P. Onnerud, E. M. E. Yeo, S. M. Haile, J. K. Stalick and J. D. Jorgensen, *Solid State Ionics*, 2000, **129**, 111.
20 C. Heremans, B. J. Wuensch, J. K. Stalick and E. Prince, *J. Solid State Chem.*, 1995, **117**, 108.
21 T. Norby, in *Diffusion and concentration of mobile species in fuel cell materials*, ed. B. Zachau-Christiansen, Proceedings Workshop, Nordic Energy Research Programme, Ås, Norway, March 1998.
22 R. Bredesen, T. Norby, A. Bardal and V. Lynum, *Solid State Ionics*, 2000, in print.
23 R. Bredesen and T. Norby, *Solid State Ionics*, 2000, **129**, 285.
24 K.-D. Kreuer, *Solid State Ionics*, 2000, **125**, 285.